Magnetic properties of σ-FeCr alloys as calculated with the charge- and spin-self-consistent KKR(CPA) method

J. Cieslak,[*] J. Tobola, S. M. Dubiel, and W. Sikora

Faculty of Physics and Applied Computer Science, AGH University of Science and Technology, al. Mickiewicza 30, 30-059 Krakow, Poland

Magnetic properties of a σ-$Fe_{16}Cr_{14}$ alloy calculated with the charge- and spin-self-consistent Korringa-Kohn-Rostoker (KKR) and combined with coherent potential approximation (KKR-CPA) methods are reported. Nonmagnetic state as well as various magnetic orderings were considered, i.e., ferromagnetic (FM) and more complex antiparallel (called APM) arrangements for selected sublattices, as follows from the symmetry analysis. It has been shown that the Stoner criterion applied to nonmagnetic density of states at the Fermi energy, E_F is satisfied for Fe atoms situated on all five lattice sites, while it is not fulfilled for all Cr atoms. In FM and APM states, the values of magnetic moments on Fe atoms occupying various sites are dispersed between 0 and 2.5 μ_B, and they are proportional to the number of Fe atoms in the nearest-neighbor shell. Magnetic moments of Cr atoms having much smaller values were found to be coupled antiparallel to those of Fe atoms. The average value of the magnetic moment per atom was found to be $\langle\mu\rangle = 0.55\mu_B$ that is by a factor of 4 larger than the experimental value found for a σ-$Fe_{0.538}Cr_{0.462}$ sample. Conversely, admitting an antiparallel ordering (APM model) on atoms situated on C and D sites, according to the group theory and symmetry analysis results, yielded a substantial reduction of $\langle\mu\rangle$ to 0.20 μ_B. Further diminution of $\langle\mu\rangle$ to 0.15 μ_B, which is very close to the experimental value of 0.14 μ_B, has been achieved with the KKR-CPA calculations by considering a chemical disorder on sites B, C, and D.

PACS number(s): 71.15.Mb, 71.20.Be, 75.20.Hr, 75.50.Bb

I. INTRODUCTION

Sigma (σ) phase has a tetragonal unit cell (type D_{4h}^{14} $P_4 2/mnm$) hosting 30 atoms distributed over five crystallographically nonequivalent sites. Due to high coordination numbers (12–15) the σ phase is a member of the Frank-Kasper family of phases. The importance of this class of structures is reinforced by the fact that they exhibit topological properties similar to simple metallic glasses due to an icosahedral local arrangement. Consequently, they can also be regarded as very good approximants for dodecagonal quasicrystals.[1] The σ phase has been revealed to occur only in such alloy systems in which at least one element is a transition metal.

Concerning the existence of the sigma phase in binary alloys, about 50 examples were found so far.[2,3] Its physical properties are characteristic of a given alloy, a high hardness and brittleness being a common feature. In the family of the binary alloy sigma phases only two, viz., Fe-Cr and Fe-V have well-evidenced magnetic properties.[4–8] In particular, the magnetic properties of σ phase strongly depend on composition. In the $Fe_{1-x}Cr_x$ system, where the σ phase exists in a narrow range of $\sim 0.45 \geq x \geq \sim 0.50$, the Curie temperature varies between 0 K (for $x \approx 0.50$) and 38 K (for $x \approx 0.45$).[6] In the Fe-V system, where the range of the σ-phase occurrence is about sixfold wider, the effect of the composition is even stronger.

Another common characteristics is a lack of stoichiometry, a feature that in combination with the complex crystallographic structure makes the σ phase a very challenging object both for theoretical investigations and interpretation of experimental data. On the other hand, the lack of stoichiometry may also have some advantage, viz., the σ phase can be

formed in a certain range of composition, giving thereby a chance for studying the influence of content on its properties, hence a possibility of tailoring these properties. For example, a magnetism of the σ phase in $Fe_{1-x}V_x$ alloys is strongly dependent on the composition and, in particular, the Curie temperature may vary between 0 K (for $x \approx 0.65$) and 320 K (for $x \approx 0.34$).[8] The complex structure and the chemical disorder (all five sites are occupied by various atoms) result in a huge number of possible atomic configurations which makes an interpretation of measurements performed by using microscopic methods, e.g., nuclear magnetic resonance or Mössbauer spectroscopy to be a difficult and often nonunique task. In these circumstances, theoretical calculations, as these presented elsewhere,[9,10] can be very helpful as they not only provide a deeper insight into the underlying physics but they also offer a very useful support for a correct interpretation of experimental data.

This paper reports theoretical calculations on the magnetic properties of the σ-FeCr system which is regarded as the archetype of all σ phases. Its magnetic properties were recently intensively investigated[6,7] and, in particular, the average magnetic moment per Fe atom was determined from magnetization measurements assuming only Fe atoms having parallel moments contribute. However, the knowledge is not complete yet, as it is unknown whether or not both types of atoms (Fe and Cr) are magnetic, and if so, what are the values of their magnetic moments on particular sublattices and what is their mutual orientation. These questions cannot be answered experimentally because one cannot grow big enough single crystals of the sigma for a decisive neutron diffraction experiment. Hence, the situation prompts and justifies further relevant theoretical calculations. The ones reported in this paper are in the line with this aim.
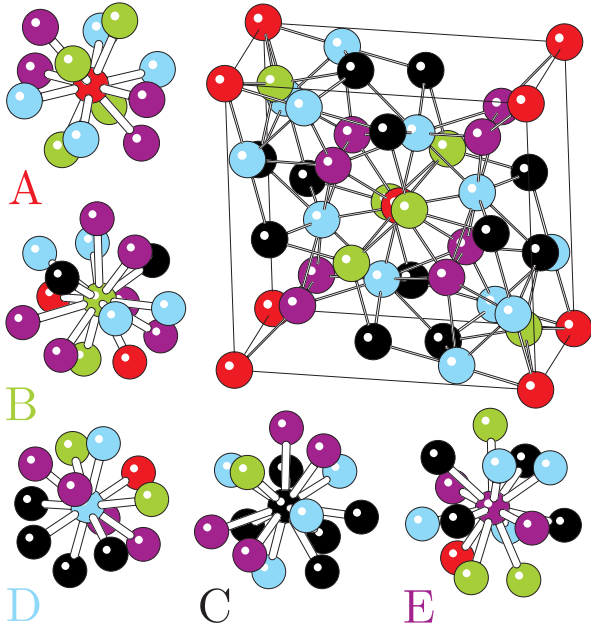
FIG. 1. (Color online) Unit cell of the σ phase. Atoms belonging to various crystallographic positions are indicated by different fillings. NN atoms of each of five lattice sites are indicated also.

II. COMPUTATIONAL DETAILS

As aforementioned, the σ phase has complex close-packed tetragonal structure with thirty atoms in the unit cell (Fig. 1). Atoms are distributed over five nonequivalent sites in the unit cell, called A, B, C, D, and E, the population of them is shown in Table I. Each position can be characterized by the total number of nearest neighbors, NNs, their distribution over five sublattices, the distances to NN atoms as well as the occupancy by Fe or Cr atoms. Some properties can be derived directly from the space-group information. Each atom in the σ-phase structure has a high coordination number (from 12 to 15 atoms), belonging to various sites (Table I). Their average interatomic distances substantially differ and are in the range from ~2.27 Å (the smallest E-E distance) to ~2.92 Å (the largest B-E distance). Interestingly, the NN spatial distribution is not far from spherical for each site (Fig. 1).

Electronic structure calculations for σ-FeCr compounds have been performed using the charge- and spin-self-consistent Korringa-Kohn-Rostoker (KKR) method. The crystal potential of the muffin-tin form has been constructed within the local-density approximation framework, applying the von Barth-Hedin formula[11] for the exchange-correlation part. With the self-consistent crystal potentials converged up to 0.1 mRy and charges up to $10^{-3}e$, total, site-decomposed and l-decomposed (s, p, and d) densities of states (DOSs) have been computed on a 601 energy point mesh for ordered models, employing the tetrahedron **k**-space integration technique (dividing the irreducible part of the Brillouin zone into 120 small tetrahedrons).

In the first stage, the electronic-structure calculations have been done for ordered approximants of the σ-FeCr alloys, and for that purpose we lowered the symmetry of the unit cell (space group $P4_2/mnm$) to a simple tetragonal one. In practice, the tetragonal unit cell and atomic positions were unchanged but variable occupancy made all 30 atomic positions crystallographically nonequivalent. In such a specified unit cell each of the crystallographic positions was occupied exclusively either by Fe or Cr atom. However, in our numerical runs we were constrained by the experimentally determined Fe/Cr concentrations on each of the five lattice sites[12] and the composition of the σ-Fe$_{16}$Cr$_{14}$, being close to the measured stoichiometry (Fe$_{0.538}$Cr$_{0.462}$), has been considered.

It should be noticed that the composition of the alloy is given in two equivalent notations. When the unit cell of the σ phase is referred to calculations, we use the Fe$_{30-x}$Cr$_x$ formula since x must be the whole number here. Conversely, the Fe$_{1-x}$Cr$_x$ formula is related to those cases, when x (the Cr concentration) in the sample was obtained experimentally.

Then, the effects of chemical disorder on the electronic structure have been studied employing the KKR method with the coherent potential approximation (CPA), which belongs to well-established techniques used in a description of intermetallic alloys. In this case, the space group $P4_2/mnm$, defining unit cell of σ phase, was allowed and five nonequivalent sites were occupied as follows: A (2i site: 100% Fe), B (4f site: 25%Fe and 75%Cr), C (8i site: 25%Fe and 75%Cr), D (8i site: 100%Fe), and E (8j site: 37.5%Fe and 62.5%Cr). The occupancies of the sublattices intentionally differed slightly from those used for the ordered approximants (although it is easy to apply precise concentrations in the KKR-CPA method) due to the fact that we intended to make possible a coherent comparison between ordered and disordered models. Thus, in the partly disordered model, Fe and Cr atoms were randomly distributed on three sites while two other sites were constrained to be fully ordered. Consequently, this model slightly differs from the experimentally determined distribution of Fe and Cr atoms in the unit cell of the σ-FeCr phase. In real samples a small fraction of chromium atoms was also detected at A and D sites (see Table II). However, we believe that the partly disordered model, forced by highly time-consuming KKR-CPA calculations, appears as a good approximation of a fully disordered σ-FeCr alloy.

In KKR-CPA calculations, the spin-dependent charge and CPA cycles have been performed self-consistently on the complex energy plane using an elliptic contour (divided into 12 sections with four Gaussian quadrature points). The KKR-CPA Green's function was computed on 75 special **k** point mesh in the irreducible part of the Brillouin zone. The Fermi energy, E_F, for all investigated alloys has been deter-

TABLE I. Atomic crystallographic positions and numbers of the nearest-neighbor atoms, NN, for the five lattice sites of the σ phase.

Site	Crystallographic positions	A	B	C	D	E	Total
				NN			
A	2i (0, 0, 0)		4		4	4	12
B	4f (0.4, 0.4, 0)	2	1	2	4	6	15
C	8i (0.464, 0.131, 0)		1	5	4	4	14
D	8i (0.74, 0.066, 0)	1	2	4	1	4	12
E	8j (0.183, 0.183, 0.252)	1	3	4	4	2	14

TABLE II. Fe site-occupation parameters of the σ-FeCr alloy, experimental and assumed for calculations. N_t stays for the percentage of the total Fe atoms on the site (referred to the 30 atoms unit cell), whereas N describes the number of Fe atoms occupying the site. N_1 and N_2 represent the values used in the calculations for ordered (KKR) and disordered (KKR-CPA) models, respectively. The corresponding relative occupancies (percentage) are given in parenthesis.

Site	N_t	N	N_1	N_2
A	11.3	1.826 (91.3)	2 (100.0)	2 (100.0)
B	6.4	1.040 (26.0)	1 (25.0)	1 (25.0)
C	20.5	3.304 (41.3)	3 (37.5)	2 (25.0)
D	44.9	7.208 (90.1)	7 (87.5)	8 (100.0)
E	17.0	2.744 (34.3)	3 (37.5)	3 (37.5)

mined from the generalized Lloyd formula,[13] which permitted us to find E_F precisely from the full derivative of the CPA Green's function (without integrating over occupied states). Like for KKR runs on ordered models of the σ-FeCr alloy, for finally converged charges and crystal potentials in the aforementioned disordered model, the KKR-CPA calculations resulted in total, site-decomposed and l-decomposed (with $l_{max}=2$) DOSs computed on a 251-energy point mesh. More details on the KKR-CPA method can be found in Refs. 14 and 15. In all our calculations, experimental crystallographic data (lattice constants and atomic positions) were employed.[9]

In order to study the magnetism of the σ-FeCr alloy spin-polarized KKR as well as KKR-CPA calculations have been performed. A collinear ordering of magnetic moments (on Fe and Cr atoms), as allowed by the employed computational codes, were assumed in a ferromagnetic (FM) state both in the ordered approximants and in the disordered alloys. However, the FM model of the σ-FeCr alloy yielded a serious discrepancy between calculated and experimental values of a total magnetization. Consequently, a more refined search for achieving a better arrangement of Fe/Cr magnetic moments, with the use of the symmetry group analysis (see Sec. III C), have been carried out. A relatively complex model of the magnetic structure, based on antiparallel alignments of the
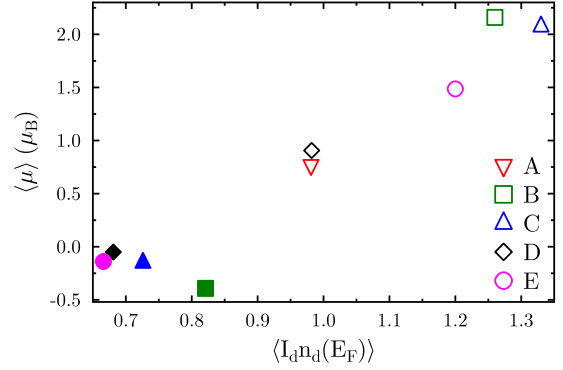

FIG. 2. (Color online) Average magnetic moments, $\langle\mu\rangle$, for five crystallographic sites versus average $\langle I_d \cdot n_d(E_F)\rangle$ value. Full symbols stand for Cr atoms while empty ones for Fe atoms.

magnetic moments within selected sublattices (called APM), was proposed and applied. Finally, spin-polarized KKR-CPA calculations were also performed for such magnetic unit cell, assuming a collinear ordering of Fe and Cr magnetic moments, only. In all figures presented throughout the paper, E_F is located at zero, and spin-polarized DOS curves are given in Ry^{-1} per spin direction.

III. RESULTS AND DISCUSSION

A. Nonmagnetic state

We start the analysis of electronic and magnetic properties of the σ-FeCr from the spin-nonpolarized calculations in order to verify the origin of magnetism in view of the Stoner model. Table III presents averaged computed values of d DOS at E_F, $n_d(E_F)$, and corresponding Stoner parameter, I_d, on all five nonequivalent sites occupied by Fe and/or Cr atoms. We see that the Stoner criterion [$I_d \cdot n_d(E_F) > 1$] is satisfied for all iron atoms ($I_d^{Fe} \sim 0.036$ Ry), being the highest one in the case of Fe at B site and the smallest one for Fe at A site. Conversely, the same condition is not fulfilled for chromium atoms ($I_d^{Cr} \sim 0.034$ Ry) essentially due to much lower DOS at E_F, which would suggest that the magnetic moments appearing on chromium atoms in the σ-FeCr alloy are in principle induced due to the presence of rather large
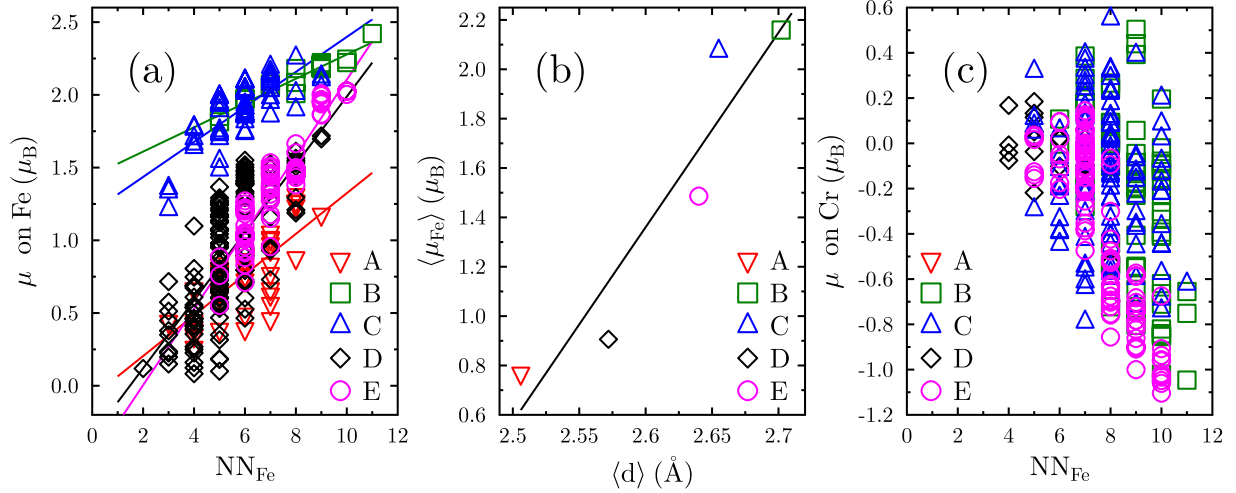
TABLE III. The average Stoner product, $S_i = \langle I_d \cdot n_d(E_F)\rangle$, ($i=$Fe,Cr) in the σ-FeCr alloy as calculated for the nonmagnetic (NM) state. Magnetic moments in μ_B of Fe and Cr atoms as well as their average values, $\langle\mu\rangle$, are indicated for various magnetic models and particular lattice sites. μ_{Fe_1} and μ_{Fe_2} in the FM model stand for the values determined in two ways described in the text. The lack of values for Cr atoms on certain sites is a consequence of the assumed distribution as presented in Table II.

Site	NM model		FM model				APM model			APM-CPA model		
	S_{Fe}	S_{Cr}	μ_{Fe_1}	μ_{Fe_2}	μ_{Cr}	$\langle\mu\rangle$	μ_{Fe}	μ_{Cr}	$\langle\mu\rangle$	μ_{Fe}	μ_{Cr}	$\langle\mu\rangle$
A	0.98		0.77	0.76		0.76	0.39		0.39	0.32		0.32
B	1.26	0.82	2.16	2.13	−0.27	0.33	2.07	−0.11	0.43	2.08	−0.10	0.44
C	1.33	0.73	2.08	1.91	−0.13	0.63	0.07	−0.06	−0.01	−2.06/+2.11	−0.11/+0.01	−0.07
D	0.98	0.68	0.91	0.90	−0.04	0.78	0.24	−0.01	0.20	−0.44/+0.65		0.21
E	1.20	0.67	1.49	1.38	−0.39	0.28	0.99	−0.20	0.25	0.90	−0.25	0.18
Av.			1.30	1.24	−0.25	0.55	0.49	−0.12	0.20	0.45	−0.16	0.15

FIG. 3. (Color online) Magnetic moments for five crystallographic sites versus the number of NN_{Fe} atoms for (a) Fe and (c) Cr. The average values of the Fe atom magnetic moments, $\langle\mu_{I_{Fe}}\rangle$, occupying different sites versus the average NN distance, $\langle d\rangle$, is shown in (b). Solid lines are the linear best fits to the data.

values of Fe magnetic moments within the NN shell. Figure 2 shows a dependence of the averaged magnetic moments calculated for the five sublattices versus the Stoner product that well supports the aforementioned experimental results, suggesting itinerant character of magnetism in this system.[7]

B. Ferromagnetic state

The aforementioned predictions from the spin-nonpolarized DOS and the Stoner product analysis have been followed by spin-polarized KKR calculations in order to determine local and average magnetic moments on Fe and Cr atoms. The magnetic structure of the σ-FeCr has not been determined yet. Hence, we first discuss the ferromagnetic ordering, being the expected upper limit of total magnetization. The values of the magnetic moments of each of 30 atoms in the unit cell obtained for the ordered approximants are presented in Fig. 3. One should notice here a relatively large dispersion of the magnetic moment of Fe atoms, μ_{Fe}, from almost 0 to nearly 2.5 μ_B. The values of μ_{Fe} for each of the five sublattices are, additionally, nicely correlated with the number of Fe atoms in the first coordination shell, NN_{Fe}. The linear correlation was described using the equation

$$\mu_{I_{Fe}} = a_I + b_I NN_{Fe} \tag{1}$$

where index $I = A, B, C, D, E$ denotes the particular sublattice.

The average value of $\mu_{I_{Fe}}$, $\langle\mu_{I_{Fe}}\rangle$, for each sublattice depends both on a_I and b_I parameters obtained from Eq. (1) fitted to the data. Using probabilities of finding particular NN_{Fe} values, $P_I(NN_{Fe})$, determined from a binomial distribution for each sublattice, $\langle\mu_{I_{Fe}}\rangle$ can be calculated with the simple formula

$$\langle\mu_{I_{Fe}}\rangle = \sum \mu_{I_{Fe}} P_I(NN_{Fe}). \tag{2}$$

As is clear from Fig. 3(b), $\langle\mu_{I_{Fe}}\rangle$ almost linearly increases with the average distances to their nearest atomic neighbors,

$\langle d\rangle$, for all sublattices. The magnetic moments on Cr atoms are much smaller and mostly oppositely aligned to those of Fe atoms. Their values range from -1.1 to 0.6 μ_B, and their correlations with the number of NN_{Fe} are much weaker than those in the case of Fe. For this reason, the average values of $\mu_{I_{Cr}}$ for various sublattices were obtained as arithmetic means of all KKR calculated values.

Since, according to the present calculations, both Fe and Cr atoms possess the magnetic moment, it seems more reasonable to express the calculated magnetization of the σ-FeCr phase, namely, the total magnetic moment of the unit cell, per one atom in the unit cell (i.e., divided by 30) rather than per Fe atom (i.e., divided by 16 in this case).

The average value of the total magnetic moment of the unit cell can be determined in two ways (Table III). (1) As the average value of just all total magnetic moments obtained in each calculation (e.g., 26 different approximants of the σ phase, involving 780 atoms). In this case, we are able to take into account the spin polarization of electrons located outside the muffin-tin spheres, giving nonvanishing contribution to total magnetization. This procedure gives 0.55 μ_B for the magnetic moments inside the muffin-tin spheres and only -0.02 μ_B for the interstitial area (0.53 μ_B in total). (2) As the sum of the weighted five $\langle\mu_I\rangle$ values, where the weights are the numbers of atoms belonging to each sublattice [Eq. (2)]. This method takes into account all possible configurations within the NN shell, even those that have not been considered in the applied model. Interestingly, the obtained value of 0.59 μ_B is quite close to the previous one.

An illustrative example of a spatial distribution of the magnetic moments of individual atoms in the unit cell is shown in Fig. 4(a). In order to present the calculated magnetic structure more clearly, the z-axis projected unit cell was doubled along x and y directions. It is worth noticing that large magnetic moments (polarized parallel) assemble to some extend. Other analyzed configurations of atoms (not shown) give qualitatively similar picture.

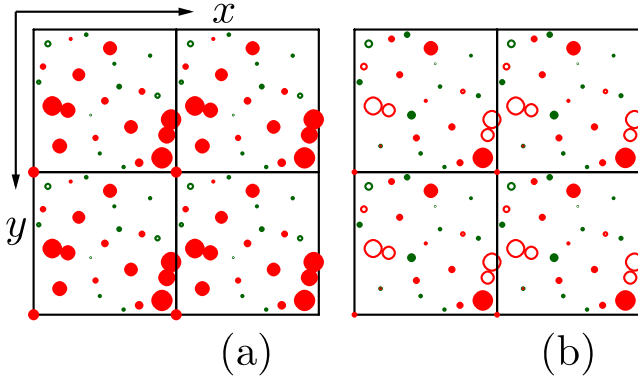Comparable results were obtained in the work of Pavlů *at*

FIG. 4. (Color online) Magnetic moments of Fe and Cr atoms in the unit cell, as seen along z axis, for (a) FM structure and (b) APM (i.e., antiparallel ordering on D and C sites) structure. Full and empty circles represent magnetic moments parallel (μ_p) and antiparall (μ_a) to the z direction, respectively. The size of red (Fe) and green (Cr) circles is proportional to the μ value.

al.[16] The authors performed spin-polarized calculations using the VASP program, considering only the sublattices fully occupied by one type of atoms. For a σ-Fe$_{0.533}$Cr$_{0.467}$ sample the total magnetic moments (per atom) found by these authors were as large as 0.52, 0.59, and 0.73 μ_B for three possible atomic configurations. Applying similar simplifications for atoms distribution in the unit cell, Kabliman et al.[17] obtained $\mu = 0.75$ μ_B (σ-Fe$_{0.60}$Cr$_{0.40}$) and 0.25 μ_B (σ-Fe$_{0.47}$Cr$_{0.53}$) using FLAPW method.

Due to the fact that these authors[16,17] reported the average values of the magnetic moments on each sublattice and also for all considered atomic configurations, their data can be directly compared with our results. As can be seen in Fig. 5, in most cases the KKR values of the magnetic moments are slightly larger than the corresponding ones reported elsewhere.[16,17] The observed difference probably results from a difference in lattice constants taken for calculations in the present work (experimental data), being slightly different

than those used in Refs. 16 and 17 (obtained from a relaxation of the unit cell). Indeed, applying the $a=b$ and c values of the lattice constants from Ref. 16, yielded smaller magnetic moments. So, the overall agreement with the previous calculations is satisfying, except for the sublattice E, where the results reported in Ref. 16 remain practically constant (1.5 μ_B for Fe) while the corresponding values obtained in the present paper are clearly NN$_{Fe}$ dependent. Actually, we observe that the magnetic moments on all five sublattices vary with NN$_{Fe}$ in more or less similar way. However, we are not aware of any particular reason for markedly different behavior of Fe and Cr magnetic moments on the E site with respect to the behavior found for other sites, as suggested in Refs. 16 and 17.

A good compatibility of the theoretical results obtained for the fully ordered systems of the σ-FeCr phase[16,17] assumed throughout the whole range of concentrations on the one hand, and those obtained for the ordered approximants of disordered system (corresponding to realistic configurations for the σ-Fe$_{0.533}$Cr$_{0.467}$ alloy) on the other, allow us to deduce the influence of the NN$_{Fe}$ on the hyperfine parameters to be weakly (if at all) dependent on the alloy stoichiometry. Therefore, the determined dependences of μ_I(NN$_{Fe}$) for each sublattice can be assumed to be valid in the whole range of the σ-FeCr existence.

The calculated average value of the magnetic moment (0.59 μ_B per atom per unit cell) should be referred to the experimental value obtained for the σ-Fe$_{0.538}$Cr$_{0.462}$, viz., $\mu = 0.14$ μ_B,[6] which is almost four times smaller than the theoretical result. Such a large and unusual discrepancy between calculated and measured values of the magnetization on one hand, as well as a nonsaturated behavior of $M(H)$ dependence[6] on the other, may indicate the magnetic structure of the σ phase is not a simple ferromagnetic one as was assumed in the aforementioned KKR calculations.
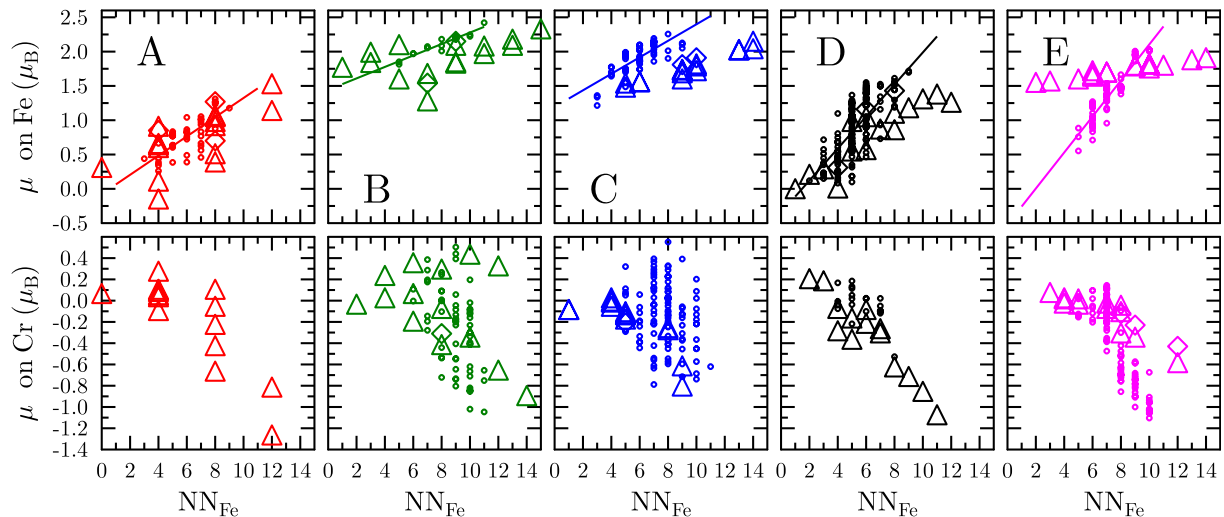

FIG. 5. (Color online) Magnetic moments of Fe and Cr atoms for five crystallographic sites versus the number of NN$_{Fe}$ atoms. Circles and solid lines stand for the KKR results (this work), whereas triangles and diamonds correspond to the calculations reported in Refs. 16 and 17, respectively.

C. Symmetry analysis and models of magnetic ordering

The large discrepancy between the theoretical (assuming FM model) and experimental results of the total magnetization in the σ-FeCr prompted us to search for a possible different magnetic ordering in such complex phase using the group theory and symmetry analysis as described below.

Let us consider an arbitrary crystal property, X, that is defined locally as $\hat{u}$, for all atomic positions in a crystal with n atoms per unit cell. The local single-site property can be a scalar, a vector (polar or axial) or even a tensor. According to the symmetry analysis method, the global quantity X can be written in the most conveniently selected basis, what usually denotes a symmetry-adapted basis, consisting of the basis vectors $\Psi_{\nu,\lambda}^{(k_L)}$ of irreducible representations (IRs) $\tau_{\nu,\lambda}^{(k)}$ of the symmetry space group, with $C_{\nu\lambda}^{(k_L)}$ as linear combination coefficients,[18]

$$X = \begin{bmatrix} \hat{u}(\vec{r}_1) \\ \hat{u}(\vec{r}_2) \\ \cdots \\ \hat{u}(\vec{r}_n) \\ \cdots \\ \hat{u}(\vec{r}_1 + \vec{t}_{p,q,s}) \\ \hat{u}(\vec{r}_2 + \vec{t}_{p,q,s}) \\ \cdots \\ \hat{u}(\vec{r}_n + \vec{t}_{p,q,s}) \end{bmatrix} = \sum_{k_L \nu \lambda} C_{\nu\lambda}^{(k_L)} \begin{bmatrix} \Psi_{\nu,\lambda}^{(k_L)}(\vec{r}_1) \\ \Psi_{\nu,\lambda}^{(k_L)}(\vec{r}_2) \\ \cdots \\ \Psi_{\nu,\lambda}^{(k_L)}(\vec{r}_n) \\ \cdots \\ \Psi_{\nu,\lambda}^{(k_L)}(\vec{r}_1)e^{i\vec{k_L}\vec{t}} \\ \Psi_{\nu,\lambda}^{(k_L)}(\vec{r}_2)e^{i\vec{k_L}\vec{t}} \\ \cdots \\ \Psi_{\nu,\lambda}^{(k_L)}(\vec{r}_n)e^{i\vec{k_L}\vec{t}} \end{bmatrix}, \quad (3)$$

$$\vec{t}_{p,q,s} = p\vec{a} + q\vec{b} + s\vec{c}, \quad (4)$$

where l, n, and λ correspond to the vectors $\mathbf{k}$, to the irreducible representations of the group, and to the IR dimensions, respectively.

In the case of any phase transition, the form of the basis vectors and the information on the representations relevant to this transition (so-called active representations) are directly given by the theory of groups and the representations. One is able to calculate these quantities using a dedicated software.[19] Then the linear combination coefficients can be determined by imposing proper conditions on the solution (specific for a given physical quantity), and the symmetry-adapted ordering modes can be found. The representation τ_ν and the coefficients $C_\lambda^{k_l,\nu}$ uniquely determine the symmetry of the structure, independently of the kind of the property taken into account. The type of the phase transition and the property under consideration are encoded in the form of the basis vectors.

In this work the symmetry analysis is applied to the structure of the σ phase described by the $P4_2/mnm$ space group, where the Wyckoff positions $2a$, $4f$, $8i$, $8i'$, and $8j$ are occupied by both Cr and Fe atoms. The aim of our analysis is to find a possible ordering of the magnetic moments that allow for a magnetic phase transition without any change in the crystal structure. As the first step, the active representations of the invariable lattice $\mathbf{k}=(0,0,0)$ for different positions and for different types of ordering (modes) have been calculated and shown in Table IV. The designations P$_1$, P$_2$,

TABLE IV. Active representations of all types of modes for $P4_2/mnm$ space group and $\mathbf{k}=0$. The meaning of the symbols is described in the text.

Site	Mode type	Representation									
		τ_1	τ_2	τ_3	τ_4	τ_5	τ_6	τ_7	τ_8	τ_9	τ_{10}
$2a$	P$_1$	1						1			
	P$_2$				1		1				2
	P$_3$			1		1				2	
$4f$	P$_1$	1						1			1
	P$_2$	1		1	1	1	1	1		1	2
	P$_3$		1	1	1	1	1		1	2	1
$8i$	P$_1$	1		1		1		1			2
	P$_2$	2	1	2	1	2	1	2	1	2	4
	P$_3$	1	2	1	2	1	2	1	2	4	2
$8j$	P$_1$	1			1		1	1		1	1
	P$_2$	2	1	1	2	1	2	2	1	3	3
	P$_3$	1	2	2	1	2	1	1	2	3	3

and P$_3$ of the mode types correspond to a scalar (change in the probability of the site occupations), polar (displacement of atoms from the equilibrium positions in the high symmetry structure), and axial (ordering of the magnetic moments) modes, respectively. Hence, for a discussion of a possible magnetic structure in the σ phase, only the latter modes are relevant. The values presented in Table IV indicate a number of different basis vector sets available for a given IR. Since the ordering of the magnetic moments is not associated with any change in the crystal structure in this system, only the models of the magnetic structure belonging to τ_1 IR are considered.

As can be seen from Table IV the ordering of the magnetic moments in this case is possible only on positions $8i$ (C and D sites) and $8j$ (E sites). The results of our calculations are given below.

Site $8i$:

$$\mu_1 = (0,0,\mu_0) = \mu_2 = \mu_3 = \mu_4 = -\mu_5 = -\mu_6 = -\mu_7 = -\mu_8.$$

Site $8j$:

$$\mu_1 = (\mu_0, -\mu_0, 0) = -\mu_2 = -\mu_7 = \mu_8,$$

$$\mu_3 = (\mu_0, \mu_0, 0) = -\mu_4 = \mu_6 = -\mu_5,$$

where the numbering of the atomic positions is given according to the International Tables for X-Ray Crystallography.[20] The parameter μ_0 is free (both in magnitude and in sign) what means that the symmetry analysis is not able to predict differences neither in values nor in relative ordering of the magnetic moments between different sublattices. Due to this freedom different models of possible magnetic orderings may be considered. However, the calculations clearly show that the arrangements of the magnetic moments within $8i$ and $8j$ sublattices are antiferromagnetic with strictly given sequences and, additionally, at $8j$ site the structure is noncollinear (four magnetic moments aligned antiparallel in the ba-
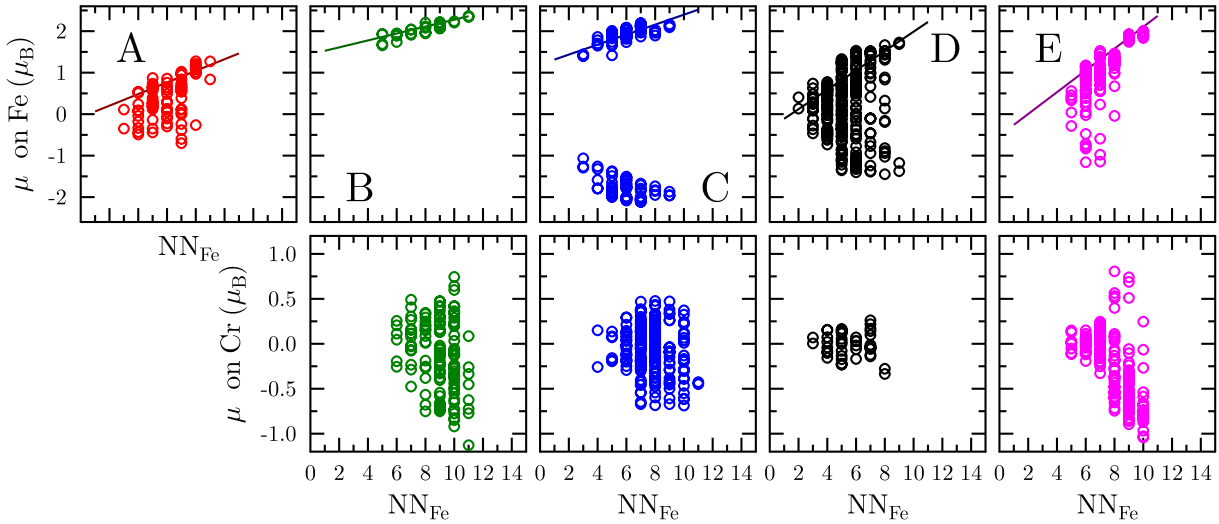
FIG. 6. (Color online) Magnetic moments of Fe and Cr atoms for five crystallographic sites versus the number of NN_{Fe} atoms as obtained with the APM model of the magnetic ordering (circles). Solid lines stand for the best fits to the magnetic moments in the FM ordering shown for the sake of comparison.

sic plane along the diagonal and four other ones also antiparallel but perpendicular to the previous moments). It is worth noticing that the purely antiferromagnetic state suggested by the aforementioned symmetry analysis is possible when atomic positions are occupied by given types of atoms with the same probability. This type of the lattice occupation is broken in the case of a Fe/Cr disordered alloy, and the proposed magnetic structures can be treated as initial conditions for the electronic-structure calculations. This is the reason why, one of the considered model of the magnetic structure, has been called APM, instead of antiferromagnetic one.

D. Ordered model of magnetic APM σ-FeCr

The KKR calculations using the APM model were performed assuming the input crystal potentials obtained for the FM state. The computations started with initial spin-polarized potentials but this fact had no effect on the finally converged APM results. Such procedure allowed us to substantially accelerate the self-consistent convergence. According to the APM model, antiferromagnetic ordering was assumed on the sublattices C and D. The symmetry analysis does not provide any information about the relative magnetic moments sequences. These sequences can be known within each sublattice separately. Consequently, two separate magnetic structures should be considered with the following relative sublattice settings: C ($\uparrow\downarrow\uparrow\downarrow$) and D ($\uparrow\downarrow\uparrow\downarrow$) as well as C ($\uparrow\downarrow\uparrow\downarrow$) and D ($\downarrow\uparrow\downarrow\uparrow$), which led us to different values of the magnetic moments. Since only collinear arrangement was allowed in the KKR calculations, antiparallel coupling of the magnetic moments on E site was not taken into account.

As is clear from Fig. 6, the assumed APM model for the Fe/Cr magnetic moment arrangement has converged to a stable magnetic configuration with atomic moments of the opposite polarization, which can be especially well seen in the case of Fe atoms located on sublattices C and D (and also

to some extent on sublattice E). Furthermore, the APM model computations have generated intermediate Fe magnetic moments with a different alignment, particularly on sublattices A and E, which were not observed for the FM ordering. There was not revealed any visible change on the sublattice B with respect to FM. The changes in the magnetic moments of Cr atoms on all sublattices have been found similar to the Fe ones. The smallest effect has been observed on the sublattice E.

In the case of APM model, the total magnetic moment as determined by averaging the moments of individual atoms yielded 0.21 μ_B, with negligible contribution (approximately -0.01 μ_B) from the outside muffin-tin volume, which ultimately gives 0.20 μ_B (Table III). This value is significantly smaller than that obtained with the FM model (0.59 μ_B), and much closer to the experimental value (0.14 μ_B).[6] This suggests that the APM ordering may be responsible for the small value of the magnetic moment deduced from the magnetization measurements.

A spatial distribution of the magnetic moments in the σ-phase unit cell found with the APM model shows a behavior similar to that detected with the FM model [see Fig. 4(b)]. In this case, however, the projected areas of the magnetic moments with the same orientation are markedly smaller.

E. Chemically disordered model for the APM ordering

Bearing in mind the aforementioned KKR results both in the FM and the APM ground states, we have also studied the effect of a chemical disorder on electronic structure and magnetic properties of the σ-$Fe_{16}Cr_{14}$ alloy using the KKR-CPA method.

In this case, the disorder (treated as random) was introduced on three sublattices (B: $Fe_{0.25}Cr_{0.75}$, C: $Fe_{0.25}Cr_{0.75}$, and E: $Fe_{0.375}Cr_{0.625}$), where the disorder is the most significant as follows from the neutron-diffraction experiment (see
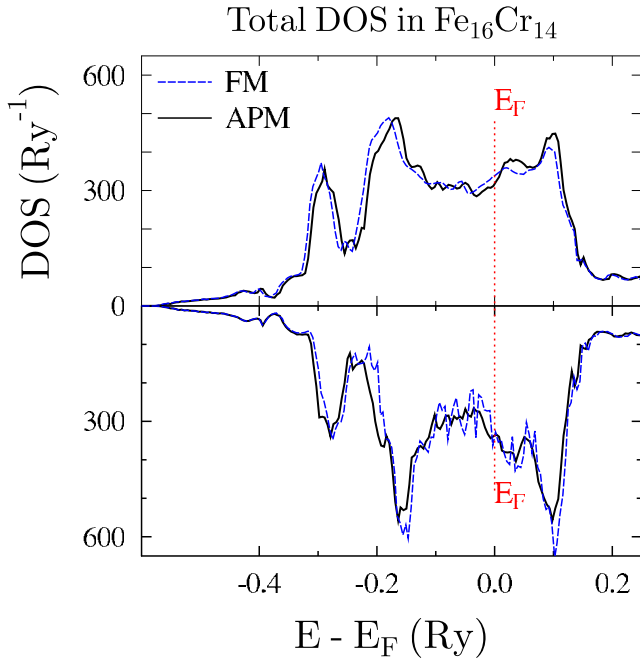
FIG. 7. (Color online) Total electronic DOS in the σ-Fe$_{16}$Cr$_{14}$ alloy obtained with the FM (blue, dashed) and APM (black, solid) models, as calculated by the KKR-CPA method.

Table II). Due to the highly time-consuming calculations, the sublattices A and D were left fully occupied by Fe atoms. This modification required to slightly decrease the Fe concentration on other sublattices, in order to maintain the Fe$_{16}$Cr$_{14}$ stoichiometry for the direct comparison between the KKR and the KKR-CPA results. The KKR-CPA results are discussed here for the FM and the APM models, neglecting the nonspin-polarized computations.

The total DOSs computed for the σ-Fe$_{16}$Cr$_{14}$ (Fig. 7) are quite similar in both cases. However, there are few subtle differences between the two presented DOS spectra. In the FM state, the DOS is more spin polarized (up DOS and down DOS are slightly shifted into lower and higher energy range, respectively) as well as two down-DOS peaks are more pronounced. This feature yields the total magnetic moment as large as ~0.4 μ_B (~12.0 μ_B per unit cell) against only ~0.15 μ_B (~4.4 μ_B per unit cell) in the APM state (Table III). Interestingly, the DOS at E_F in the APM state is a bit smaller than that in the FM one, which may tentatively support a better stability of the APM state, relative to the FM one. Before inspecting in more detail the local origin of the magnetism in the disordered σ-Fe$_{16}$Cr$_{14}$ alloy, let us remark that disorder effects markedly decrease the magnetic moments on Fe atoms on all sublattices and, in consequence, the total magnetization per unit cell. This feature is well seen for the FM state, where the value of 0.4 μ_B was calculated with KKR-CPA for the total magnetization, compared to almost 0.6 μ_B with KKR as obtained via averaging over a set of results obtained for the ordered approximant approach. Quite similar behavior was found for the APM state since the magnetization values gained from the KKR-CPA and the KKR methods also differ (0.15 μ_B for disordered alloy against 0.20 μ_B for ordered models of the σ-Fe$_{16}$Cr$_{14}$). Hence, an
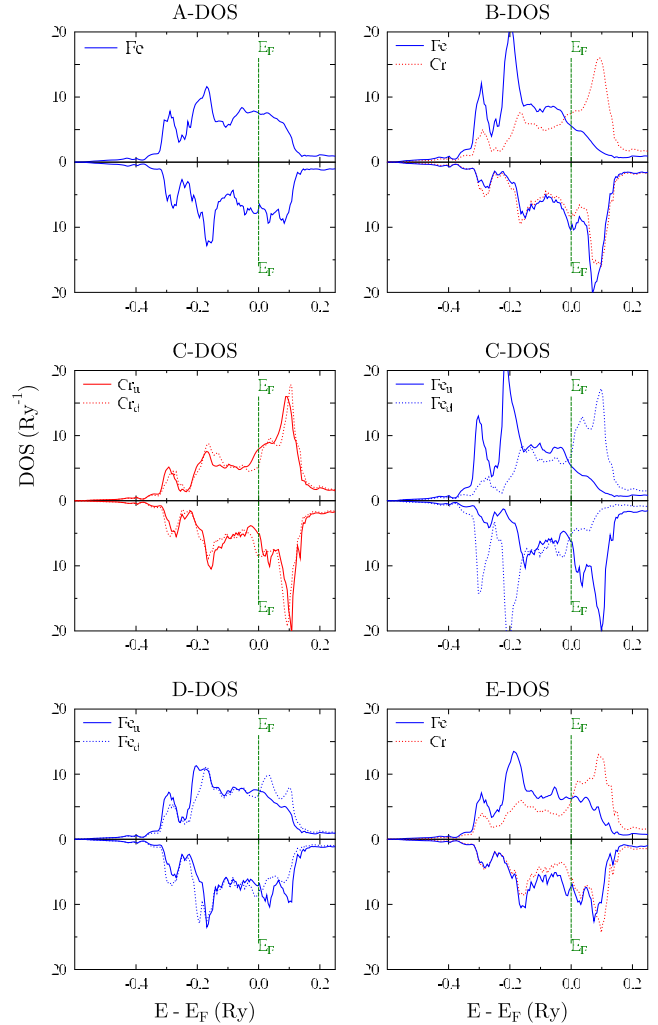

FIG. 8. (Color online) Site-decomposed KKR-CPA DOS for the σ-Fe$_{16}$Cr$_{14}$ alloy as obtained with the APM model.

inclusion of the chemical disorder into the electronic-structure calculations has additionally lowered the total magnetization by about 25%.

The choice of the APM magnetic structure for the KKR-CPA calculations has resulted in the total magnetic moment (0.15 μ_B) in an excellent agreement with the experimental data (0.14 μ_B) for the σ-Fe$_{0.538}$Cr$_{0.462}$ alloy. It should be added that in the APM model, according to the symmetry analysis, sites C and D with multiplicity 8 were split into two "subsites," each with multiplicity 4, having an antiparallel orientation. Consequently, in order to distinguish the magnetic moments and DOSs of Fe atoms on D site and those of Fe/Cr atoms on C site that are arranged parallel or antiparallel to other sites, (A, B, and E), we have introduced indexes u and d, respectively.

Inspecting the Fe DOSs on all sites in the APM state (Fig. 8), one can notice two sites (B and C) with strongly polarized electronic spectrum, giving rise to large local magnetic moments of +2.08 μ_B (B site) as well as of −2.06 μ_B (Fe$_d$) and of +2.11 μ_B(Fe$_u$) on C site. The spin polarization of DOS on other sites remains much smaller, resulting in relatively lower values of Fe magnetic moments

on A (+0.32 μ_B), D (−0.44 on Fe_d and +0.65 μ_B on Fe_u) and E (+0.90 μ_B). The KKR-CPA results well reflect the aforementioned correlation (Sec. III B) between the values of the Fe magnetic moment and the average distance to NN atoms, well supporting the KKR findings for the ordered approximants. It is worth noticing that on these sites, where Cr atoms were substituted (B, C, and E), a small Cr magnetic moment was found to be always aligned antiparallel to the Fe magnetic moment on the same site. Such electronic-structure behavior was also found for the FM state using the KKR-CPA method. As already mentioned, the polarization of the Cr DOS is weak and for E site a slight DOS asymmetry for two spin directions yielded the magnetic moment of about −0.20 μ_B. In the case of B and C sites, the calculated Cr magnetic moment is as small as −0.10 μ_B, on average. At present, we must rely on the above described interpretation of the magnetic ordering in the σ-FeCr system since first the APM structure appears the simplest one and second there are no available experimental evidences indicating more complex (e.g., noncollinear) magnetic structure.

IV. CONCLUSIONS

The results of the electronic-structure calculations using KKR and KKR-CPA methods reported in the present study can be summarized. Both Fe and Cr atoms in the σ-$Fe_{16}Cr_{14}$ alloy are magnetic. Magnetic moments of Fe atoms for each lattice site linearly increase with the number of Fe atoms in the nearest-neighbor shell, NN_{Fe}, whereas Cr atoms are coupled antiparallel with respect to Fe atoms (values of the magnetic moments for both Fe and Cr atoms are characteristic of a given lattice site). Ferromagnetic ordering of the Fe-site magnetic moments accounted for the calculations results in a significant overestimation of the magnetism in the investigated sample. Fortunately, admission of an antiparallel ordering on some selected sites, suggested by the symmetry analysis, in a combination with a partial chemical disorder yields the excellent agreement with the experimentally found value of the average magnetic moment per atom.

*Corresponding author; cieslak@novell.ftj.agh.edu.pl

[1] S. I. Simdyankin, S. N. Taraskin, M. Dzugutov, and S. R. Elliott, Phys. Rev. B **62**, 3223 (2000).

[2] E. O. Hall and S. H. Algie, Metall. Rev. **11**, 61 (1966).

[3] J.-M. Joubert, Prog. Mater. Sci. **53**, 528 (2008).

[4] D. A. Read, E. H. Thomas, and J. B. Forsyth, J. Phys. Chem. Solids **29**, 1569 (1968).

[5] Y. Sumitomo, T. Moriya, H. Ino, and F. E. Fujita, J. Phys. Soc. Jpn. **35**, 461 (1973).

[6] J. Cieślak, M. Reissner, W. Steiner, and S. M. Dubiel, J. Magn. Magn. Mater. **272-276**, 534 (2004).

[7] J. Cieślak, M. Reissner, W. Steiner, and S. M. Dubiel, Phys. Status Solidi **205**, 1794 (2008).

[8] J. Cieślak, B. F. O. Costa, S. M. Dubiel, M. Reissner, and W. Steiner, J. Magn. Magn. Mater. **321**, 2160 (2009).

[9] J. Cieslak, J. Tobola, S. M. Dubiel, S. Kaprzyk, W. Steiner, and M. Reissner, J. Phys.: Condens. Matter **20**, 235234 (2008).

[10] J. Cieslak, J. Tobola, and S. M. Dubiel, Phys. Rev. B **81**, 174203 (2010).

[11] U. von Barth and L. Hedin, J. Phys. C **5**, 1629 (1972).

[12] J. Cieslak, M. Reissner, S. M. Dubiel, J. Wernisch, and W. Steiner, J. Alloys Compd. **460**, 20 (2008).

[13] S. Kaprzyk and A. Bansil, Phys. Rev. B **42**, 7358 (1990).

[14] A. Bansil, S. Kaprzyk, P. E. Mijnarends, and J. Tobola, Phys. Rev. B **60**, 13396 (1999).

[15] T. Stopa, S. Kaprzyk, and J. Tobola, J. Phys.: Condens. Matter **16**, 4921 (2004).

[16] J. Pavlů, J. Vřešťál, and M. Šob, Intermetallics **18**, 212 (2010).

[17] E. A. Kabliman, A. A. Mirzoev, and A. L. Udovskii, Phys. Met. Metallogr. **108**, 435 (2009).

[18] Yu. A. Izyumov and V. N. Syromyatnikov, *Phase Transitions and Crystal Symmetry* (Kluwer Academic, Dordrecht, 1990).

[19] W. Sikora, F. Bialas, and L. Pytlik, J. Appl. Crystallogr. **37**, 1015 (2004).

[20] T. Hahn, *International Tables For Crystallography* (The International Union of Crystallography/Springer, The Netherlands, 2005).